

# Investigation of Nonelastic Response of Semicrystalline Polymers at High Strain Levels

A. PEGORETTI, A. GUARDINI, C. MIGLIARESI, T. RICCO

Department of Materials Engineering, University of Trento, Via Mesiano 77, 38050 Trento, Italy

Received 8 July 1999; accepted 25 February 2000

**ABSTRACT:** The nonelastic behavior at high strains of three semicrystalline polymers [i.e., nylon-6, poly(ethylene terephthalate), and poly(ethylene 2,6-naphthalenedicarboxylate)] was investigated. For all materials, room temperature tensile strain recovery tests revealed the existence of two components of nonelastic deformation: a fast-relaxing component (called anelastic) and a slow-relaxing component (usually called plastic). A strain recovery master curve could be constructed for each material from the strain recovery data obtained at various temperatures. The shift factors versus temperature relationship for the strain recovery master curves allowed us to evaluate an activation energy for the nonelastic strain recovery process. These data were then compared with the activation energy for the glass-transition process evaluated by dynamic mechanical measurements at low strain. The aim of this comparison was to investigate the influence of viscoelasticity on the nonelastic deformation recovery. © 2000 John Wiley & Sons, Inc. *J Appl Polym Sci* 78: 1664–1670, 2000

**Key words:** nonelastic deformation; semicrystalline polymers; viscoelasticity

## INTRODUCTION

Studies on yield and postyield behavior of amorphous glassy polymers<sup>1–10</sup> show the existence of two distinct nonelastic strain components. In particular, when the material is deformed in the glassy state, one can distinguish between an anelastic ( $\epsilon_{an}$ ) component that can recover in a certain interval of time, even at a temperature well below the glass transition, and a permanent plastic ( $\epsilon_{pl}$ ) component. However, experimental evidence<sup>1,4,5,10</sup> proved that this so-called plastic deformation is actually reversible upon heating up to or above the glass-transition temperature ( $T_g$ ). The different nature of associated molecular movements determines distinct time ranges for

the recovery of the two strain components at temperatures far below the glass transition (i.e., at  $T < T_g - 20^\circ\text{C}$ ).<sup>4,5</sup> A molecular model by Perez et al.<sup>11–14</sup> suggests a “crystal-like” mechanism in which the primary effect of strain in the glassy state is the nucleation of localized shear-induced defects called shear microdomains (SMDs), which are associated with an  $\epsilon_{an}$ . The growth of SMDs determines a borderline constraint in the surrounding undeformed matrix, which is responsible for strain recovery upon unloading. The eventual appearance of an  $\epsilon_{pl}$  is determined by the interaction of two or more SMDs, thus causing molecular rearrangements, which annihilate the anelastic component and produce plasticity.<sup>1,2–4</sup>

Most past works concentrated on the characterization of yield and postyield behavior of amorphous polymers, in particular poly(methyl methacrylate) (PMMA), atactic polystyrene (a-PS), and polycarbonate (PC). The aim of the present work was to investigate the characteristic features of nonelastic deformation recovery pro-

Correspondence to: A. Pegoretti (Alessandro.Pegoretti@ing.unitn.it).

Contract grant sponsor: Consiglio Nazionale delle Ricerche, Rome.

*Journal of Applied Polymer Science*, Vol. 78, 1664–1670 (2000)  
© 2000 John Wiley & Sons, Inc.

cesses in semicrystalline polymers like nylon-6 (PA6), poly(ethylene terephthalate) (PET), and poly(ethylene 2,6-naphthalenedicarboxylate) (PEN).

## EXPERIMENTAL

### Materials

Three different semicrystalline polymeric films were analyzed: PA6, PET, and PEN. The PA6 film had a thickness of 45  $\mu\text{m}$  and was provided by Snia S.p.A. (Milan, Italy). The 52  $\mu\text{m}$  thick PET film was a commercial product (Mylar<sup>®</sup>) from Du Pont. The PEN film was provided by Hoechst-Trevira as a commercial film (Polyclear<sup>®</sup> N100) whose thickness was 100  $\mu\text{m}$ . All the experiments were performed on samples obtained along the machine direction of the extruded films.

### Tensile Tests

Monotonic tensile tests were performed on all materials with an Instron 4502 tensile tester equipped with a 10-kN load cell. The strain rate was 0.1/min on 300  $\times$  10 mm (length  $\times$  width) rectangular samples, which followed ASTM Standard D 882-91.

### Differential Scanning Calorimetry (DSC)

A Mettler DSC 30 DS calorimeter was used to detect the melting temperature ( $T_m$ ) of the crystalline domains. Measurements were performed on specimens with a weight of about 20 mg at a heating rate of 10°C/min in a nitrogen flux of 100 mL/min. The crystallinity percentage ( $X_c$ ) was assessed by integrating the normalized area of the endothermal peak and rating the heat involved to the reference value of the 100% crystalline polymer: 190 J/g for PA6,<sup>15</sup> 140 J/g for PET,<sup>16</sup> and 104 J/g for PEN.<sup>17</sup> The glass-transition temperature of the amorphous region was hardly or not detectable on the DSC traces.

### Dynamic Mechanical Thermal Analysis (DMTA)

A Polymer Laboratories Ltd. MkII dynamic thermal analyzer was used in the tensile configuration on 4  $\times$  20 mm (width  $\times$  length) samples of the film. Tests were performed at a heating rate of 0.4°C/min at frequencies of 0.3, 1, 3, 10, 30, and 50 Hz. A peak to peak displacement of 64  $\mu\text{m}$  was set in order to apply a small strain amplitude (in any case lower than 0.4%). The glass-transition

**Table I Elastic Modulus ( $E$ ) Crystallinity Content ( $X_c$ ), Melting Temperature ( $T_m$ ), and Glass-Transition Temperature ( $T_g$ ) of Materials**

Material	Thickness ( $\mu\text{m}$ )	$E$ (MPa)	$X_c$ (%)	$T_m$ (°C)	$T_g$ (°C)
PA6	45	1400	28	221	69
PET	52	4500	36	260	105
PEN	100	5150	44	269	143

temperature was evaluated as the  $\tan \delta$  peak temperature at a test frequency of 0.3 Hz.

### Strain Recovery Tests

Loading–unloading strain cycles were performed by using an Instron model 4502 machine equipped with a 100-N cell. The constant strain rate was 0.1/min. Rectangular specimens (130  $\times$  8 mm length  $\times$  width) were loaded up to a strain of 20% and unloaded at the same crosshead speed. The residual strain ( $\epsilon_{\text{res}}$ ) was evaluated on samples after unloading. Two marks were made with a felt tip pen on the surface of the undeformed samples and the distance ( $l_0$ ) between them was measured with an optical transmission microscope (Leitz model Ortholux II POL-BK). The distance between the two marks was successively monitored after various time intervals ( $t_{\text{rec}}$ ) by positioning the specimens under the microscope, thus calculating a residual strain as

$$\epsilon_{\text{res}} = \frac{l - l_0}{l_0} \quad (1)$$

Strain recovery tests at increasing temperatures ( $T_{\text{rec}}$ ) were performed on samples deformed with the Instron machine and then positioned (after a standard time of 2.5 min) in a small thermostatic chamber located under the microscope. It is worth noting that no shrinkage was found on undeformed samples kept for 2 h at the highest recovery temperature.

## RESULTS AND DISCUSSION

A summary of values of some properties measured on the PA6, PET, and PEN films is given in Table I. Note that the selected materials are characterized by increasing values of the tensile modulus and melting and glass-transition tempera-

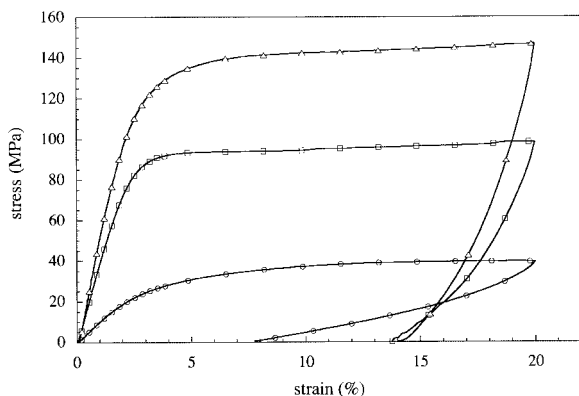


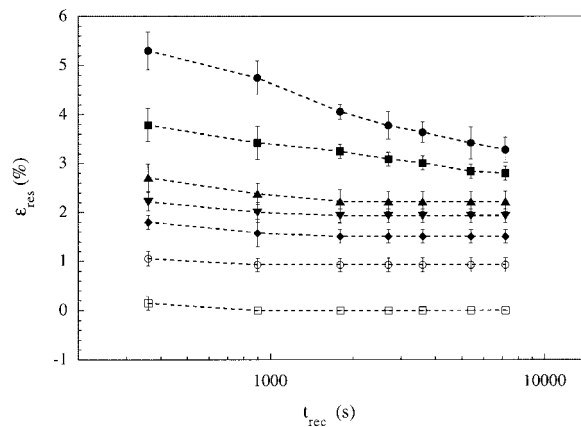
**Figure 1** Stress–strain curves of (○) PA6, (□) PET, and (△) PEN films deformed up to 20% strain and unloaded.

tures. The crystal melting temperature evaluated with the DSC measurements for all the materials under investigation was not appreciably affected by the deformation up to 20%.

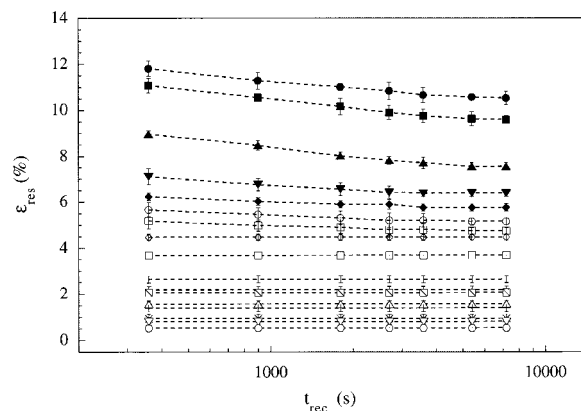
A comparison of the stress–strain curves of the materials deformed up to 20% and then unloaded is reported in Figure 1.

After unloading,  $\epsilon_{\text{res}}$  was monitored as a function of  $t_{\text{rec}}$  at various  $T_{\text{rec}}$ . Experimental data for PA6 and PEN are reported in Figure 2(a,b) respectively, while similar results obtained on the PET films were already presented.<sup>18</sup> These figures show how strain recovery proceeds during the time at various temperatures. In any case, strain recovery data at room temperature (25°C) shows two components of nonelastic strain: an anelastic fast recovering component  $\epsilon_{\text{an}}$ , and an apparently permanent plastic component  $\epsilon_{\text{pl}}$ . At this point the distinction between the two components can be made on the basis of different recovery speeds at temperatures far below the  $T_g$  of the materials. Tests at increasing recovery temperatures show that the strain recovering phenomenon accelerates, thus evidencing the reversible nature of both components upon heating. In fact, for all the investigated materials, a sufficiently high temperature near or above the  $T_g$  determines a complete strain recovery. The speed at which both components recover at high temperature is such that anelastic and plastic recovery are no longer distinguishable. Similar to the behavior of fully amorphous polymers,<sup>1–10</sup> the thermomechanically activated nature of strain recovery for semicrystalline polymers can be seen. Experimental data points at  $T_{\text{rec}} > 25^\circ\text{C}$  were corrected by subtracting the specimen thermal

expansion evaluated by using the following coefficients of linear thermal expansion:  $\alpha_T = 9 \times 10^{-5}/^\circ\text{C}$  for PA6<sup>15</sup> and  $1.7 \times 10^{-5}/^\circ\text{C}$  for PET<sup>19</sup> and PEN. Comparing the behavior of the three materials under investigation, it is worth noting that at any given temperature the recovery degree is a function of the difference between the recovery and glass-transition temperatures. In other words, after equal recovery times,  $\epsilon_{\text{res}}$  is higher as the difference between  $T_g$  and  $T_{\text{rec}}$  increases. At this point a first distinction from the amorphous polymers can be made by observing that in the semicrystalline polymers a complete recovery is possible only at temperatures above the  $T_g$  while for amorphous polymers heating up to the  $T_g$  is usually sufficient.<sup>4</sup>



(a)



(b)

**Figure 2** (a) Strain recovery curves for PA6 film at  $T_{\text{rec}}$  of (●) 25, (■) 30, (▲) 50, (▼) 55, (◆) 60, (○) 70, and (□) 75°C. The error bars represent the standard deviation of the measured values. (b) Strain recovery curves for PEN film at  $T_{\text{rec}}$  of (●) 25, (■) 40, (▲) 50, (▼) 60, (◆) 70, (○) 80, (□) 90, (◇) 100, (◻) 110, (|) 120, (–) 130, (◻) 140, (△) 150, (+) 160, (×) 170, (▽) 180, and (⊙) 190°C.

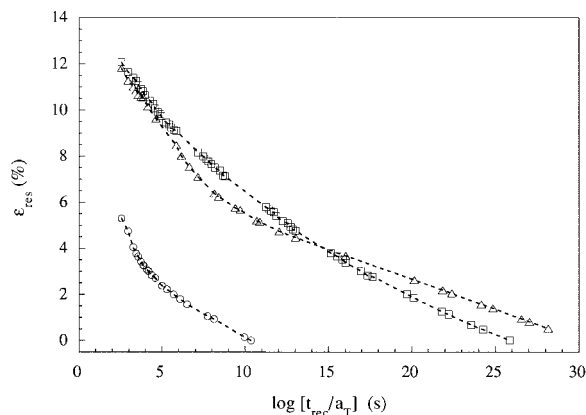


**Figure 3** Strain recovery master curves at  $T_0 = 25^\circ\text{C}$  for (○) PA6, (□) PET, and (△) PEN films, where  $a_T$  is the appropriate shift factor.

Strain recovery master curves were built on the basis of a time–temperature superposition principle<sup>20</sup> by horizontally shifting the points relative to  $T_{\text{rec}} > T_0 = 25^\circ\text{C}$ . The results reported in Figure 3 clearly show how a nearly complete recovery of the  $\varepsilon_{\text{an}}$  and  $\varepsilon_{\text{pl}}$  components could occur spontaneously after a certain lapse of time. The complete recovery occurs faster for the polyamide than for PET and PEN films. All curves show a gradually slowing recovery, which does not allow a direct distinction between anelastic and plastic recovery time ranges on the basis of the strain recovery master curves. To distinguish the anelastic from the plastic recovery, the derivative of the residual strain with the logarithm of time was calculated with a simple finite increment differentiation. The result was a distribution of recovery times, which also showed the gradually decreasing trend shown in Figure 4(a,b) for PA6 and PEN, respectively. The time recovery distribution data for PET, reported in a previous work,<sup>18</sup> had a similar trend. In the amorphous polymers a similar procedure showed the existence of a distribution characterized by the presence of two distinct peaks<sup>1–4</sup>: one spread peak at low recovery times and a second concentrated peak at high recovery times, which were separated by an interval in which the distribution went to zero. Physically, on a time–temperature equivalence basis, this corresponds to an anelastic recovery over a wide range of temperatures below the  $T_g$ , while a complete plastic recovery happens at temperatures around the  $T_g$ . In the semicrystalline polymers examined in this work, no clear distinction was possible on the basis of only the time distribution curves. This character-

istic feature of the semicrystalline polymers could be explained on the basis of their microstructure. In fact, the presence of crystals very likely determines the existence of a gradient of mobility between the amorphous and crystalline phases.<sup>21,22</sup> Consequently, passing from the crystal habit to the amorphous matrix, the corresponding decreasing values of the local  $T_g$  could cause a widespread distribution of the characteristic recovery times. On a double logarithmic scale, the strain recovery master curves allow the appreciation of the existence of two time ranges with different recovery speeds separated by a knee: at low recovery times a faster recovery kinetic refers to the anelastic component; at higher recovery times the process slows down with plastic component recovery. The transition point between the two ranges was fixed as the intersection of the two lines resulting from a linear fit of the two parts of the recovery master curves. This procedure allowed

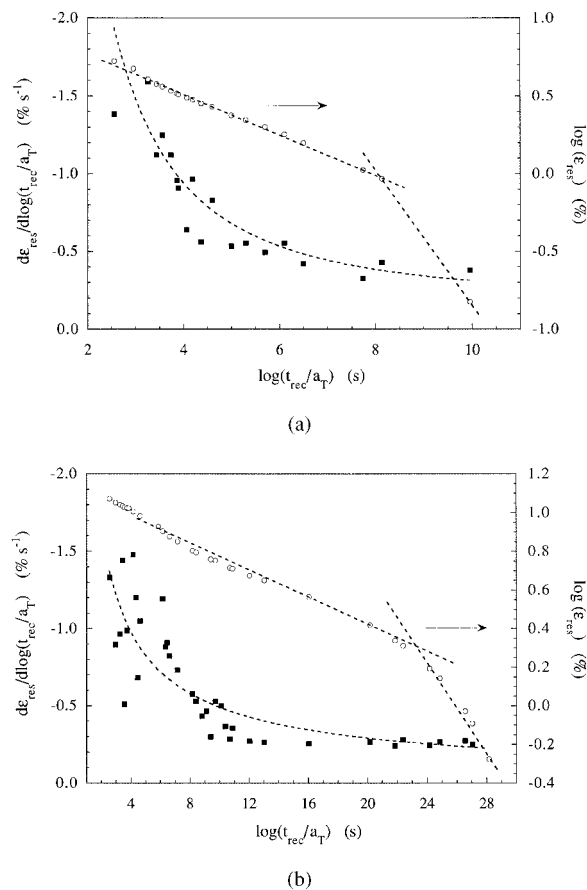


**Figure 4** (a) Recovery time distribution,  $d\varepsilon_{\text{res}}/[d \log(t_{\text{rec}}/a_T)]$ , and strain recovery master curves at  $T_0 = 25^\circ\text{C}$  on a double logarithmic scale for (a) the PA6 films and (b) the PEN films.

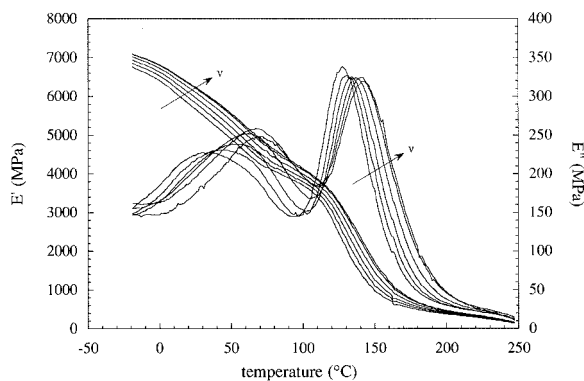


**Figure 5** Dynamic storage modulus ( $E'$ ) and loss modulus ( $E''$ ) curves as a function of temperature at frequencies ( $\nu$ ) of 0.3, 1, 3, 10, 30, and 50 Hz for the PEN film.

us to fix a value for every material of the characteristic time for a complete anelastic recovery at  $\varepsilon_0 = 20\%$  and  $T_{\text{rec}} = 25^\circ\text{C}$ . These characteristic times increased as the material glass transition increased and were about  $10^8$ ,  $10^{18}$ , and  $10^{23}$  s for PA6, PET, and PEN, respectively.

More information about the viscoelastic nature of the deformational mechanism above the yield point emerged from the DMTA. The storage and loss moduli of the various films were measured in a linear viscoelastic regime for strains lower than 0.4% at frequencies of 0.3–50 Hz in a wide temperature range. A typical result is reported in Figure 5 for PEN. The storage modulus data were subsequently rearranged by a standard time–temperature superposition principle in order to obtain the master curves reported in Figure 6. The temperature dependence of the shift factors for both the strain recovery and  $E'$  master curves are compared in Figure 7(a,b). The same situation occurred for the PET film as reported in a previous study.<sup>18</sup> The activation energies were calculated using an Arrhenius equation for the linear parts of the curves below the glass transition, where the shift factor passes from a glassy to a rubbery state. For the sake of comparison, the activation energy for the glass transition was also evaluated by considering the frequency–temperature dependence of the loss modulus peaks,  $\nu_{\text{peak}}$ . This is usually expressed by an Arrhenius type equation as follows:

$$\nu_{\text{peak}} = A \exp\left(\frac{-\Delta E}{RT}\right) \quad (2)$$

where  $\Delta E$  is the activation energy for relaxation, corresponding to the energy barrier for polymer

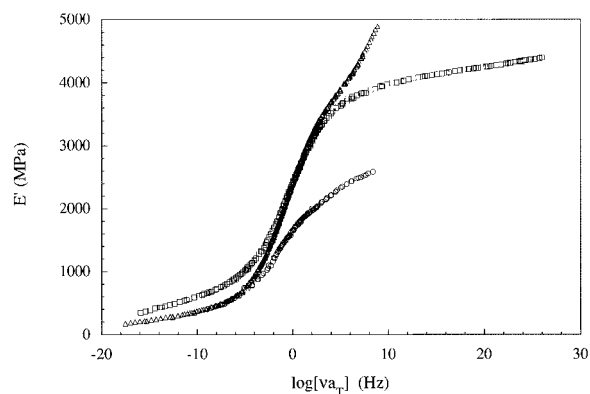
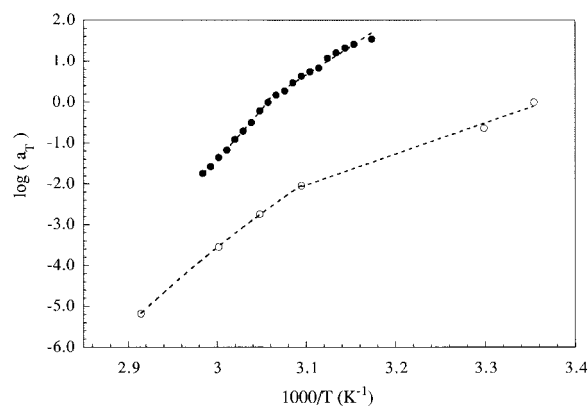
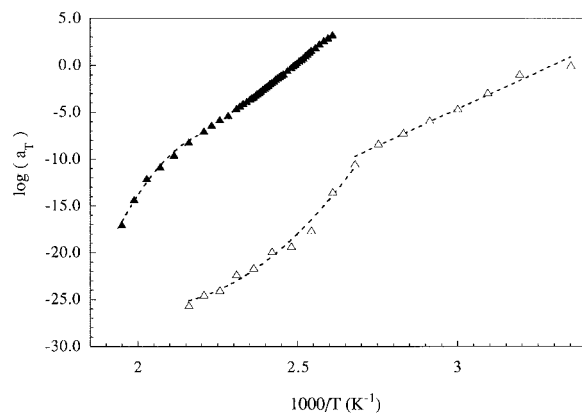


**Figure 6** Dynamic storage modulus master curves for (○) PA6 at  $T_0 = 54^\circ\text{C}$ , (□) PET at  $T_0 = 98^\circ\text{C}$ , and (△) PEN at  $T_0 = 129^\circ\text{C}$ .



(a)



(b)

**Figure 7** (a) A comparison of shift factors for (○) strain recovery and (●) dynamic storage modulus master curves for PA6. (b) A comparison of shift factors for (△) strain recovery and (▲) dynamic storage modulus master curves for PEN.

chain movement from one site to another. Figure 8 presents examples of Arrhenius plots for the glass transitions of PA6, PET, and PEN films whose slopes produced the activation energy.

The activation energy values, which were obtained in several different ways, are reported in Figure 9 as a function of the glass-transition temperature of the materials. It is interesting to observe that the activation energies increase as the  $T_g$  increases and the activation energies for the strain recovery are systematically lower than those obtained from the DMTA data. Moreover, the glass-transition temperatures, indicated by the transition point in the shift factor curves reported in Figure 7, seem to markedly differ for the two cases, being lower for the strain recovery experiments. This was tentatively explained as a consequence of the molecular relaxations processes involved in the appearance and growth of SMDs.<sup>20</sup> These are typically intramolecular and of a  $\beta$ -activated nature, and the rotation of sections of the molecular chain are under the effect of a component of shear stress. Subsequently,  $\alpha$ -activated intermolecular rearrangements are possible for the interaction of the borderline of two or more SMDs. The result is the presence of hybrid  $\alpha/\beta$ -activated states in the glassy strained matrix, which shift the lower part of the  $\alpha$ -relaxation peak toward lower temperatures.<sup>23</sup> In the semicrystalline polyamide and polyesters the  $\alpha$  relaxation coincides with the glass transition. A secondary effect of this could be the lower value of the activation energy for the strain recovery experiments.

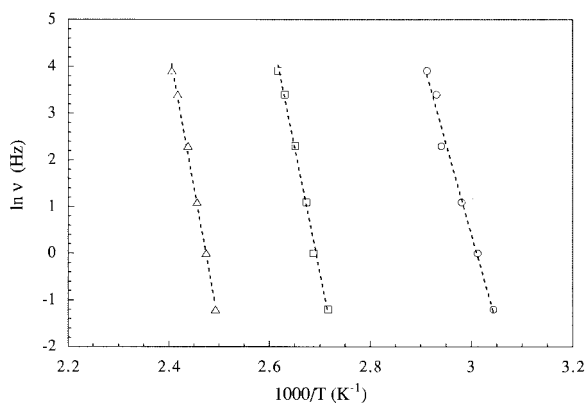


**Figure 8** Arrhenius plot for the activation energy evaluation for the  $\alpha$ -relaxation process in (○) PA6, (□) PET, and (△) PEN films.

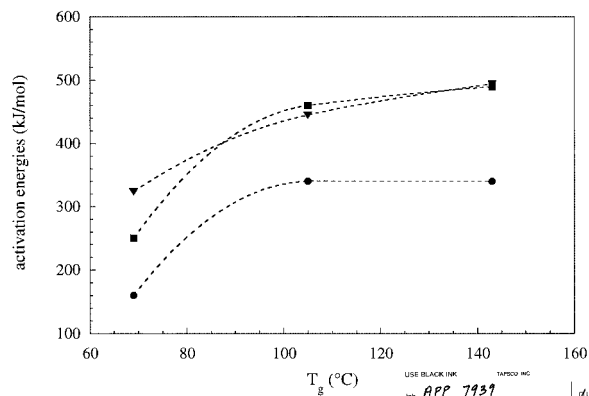


**Figure 9** Activation energies for (●) strain recovery and the glass-transition process from (■)  $E'$  master curve shift factors and (▼)  $\tan \delta$  peaks Arrhenius plot as a function of the polymer glass-transition temperatures.

## CONCLUSIONS

The nonelastic deformation of semicrystalline polymers was studied. Strain recovery tests performed at various temperatures evidenced that, similar to the amorphous polymers, two components of nonelastic deformation (anelastic and plastic) can be distinguished on the basis of their characteristic recovery times. For each selected material, a strain recovery master curve was then constructed, thus permitting the estimation of the time necessary for a complete recovery of nonelastic deformation. Nonelastic deformation of samples deformed up to 20% were entirely recovered in a few minutes at a temperature about 40–50°C higher than the  $T_g$  for all the materials under investigation. It is important to emphasize that heating amorphous polymers up to the  $T_g$  is sufficient for a complete recovery.

## REFERENCES

- Oleinik, E. F. In *High Performance Polymers: Structure, Properties, Composites, Fibers*; Baer, E.; Moet, A., Eds.; Hanser: Munich, 1991; p 79.
- Oleinik, E. F.; Salamatina, O. B.; Rudnev, S. N.; Shenogin, S. V. *Polym Sci Ser A* 1993, 35, 1532.
- Salamantina, O. B.; Höhne, G. W. H.; Rudnev, S. N.; Oleinik, E. F. *Thermochim Acta* 1994, 247, 1.
- Quinson, R.; Perez, J.; Rink, M.; Pavan, A. *J Mater Sci* 1996, 31, 4387.
- David, L.; Quinson, R.; Gauthier, C.; Perez, J. *Polym Eng Sci* 1997, 37, 1633.
- Hasan, O. A.; Boyce, M. C. *Polymer* 1993, 34, 5085.

7. Hasan, O. A.; Boyce, M. C.; Li, X. S.; Berko, S. *J Polym Sci Part B Polym Phys* 1993, 31, 185.
8. Hasan, O. A.; Boyce, M. C. *Polym Eng Sci* 1995, 35, 331.
9. Chang, B. T.; Li, J. C. M. *Polym Eng Sci* 1988, 28, 1198.
10. Kung, T. M.; Li, J. C. M. *J Mater Sci* 1987, 22, 3620.
11. Mangion, M. B. M.; Cavaille, J. Y.; Perez, J. *Phil Mag A* 1992, 66, 773.
12. Perez, J. *Physique et Mecanique des Polymers Amorphes*; Lavoisier: Paris, 1992.
13. Perez, J.; Cavaille, J. Y.; Etienne, S.; Fouquet, F. *J Phys* 1980, 41, C8.
14. Perez, J. *Rev Phys Appl* 1986, 21, 93.
15. Pflüge, R. In *Polymer Handbook*, 3rd ed.; Brandrup, J.; Immergut, E. H., Eds.; Wiley: New York, 1989; Vol. 112.
16. Mehta, A.; Gaur, U.; Wunderlich, B. *J Polym Sci Part B Polym Phys* 1978, 16, 289.
17. Cheng, S. Z. D.; Wunderlich, B. *Macromolecules* 1988, 21, 789.
18. Pegoretti, A.; Guardini, A.; Migliaresi, C.; Ricco, T. *Polymer* 2000, 41, 1857.
19. Heffelfinger, C. J.; Knox, K. L. In *The Science and Technology of Polymer Films*; Sweeting, O. J., Ed.; Wiley-Interscience: New York, 1971; Vol. 11, p 587.
20. Ferry, J. D. *Viscoelastic Properties of Polymers*; Wiley: New York, 1980.
21. McCrum, N. G.; Read, B. E.; Williams, G. *Anelastic and Dielectric Effects in Polymeric Solids*; Dover Publications Inc.; New York, 1967.
22. Struik, L. C. E. *Physical Aging in Amorphous Polymers and Other Materials*, Elsevier: Amsterdam, 1978; p 55.
23. Quinson, R.; Perez, J.; Germain, Y.; Murraciale, J. M. *Polymer* 1995, 36, 743.